Possible Wavelength Range Extension of the TESLA Test Facility Free Electron Laser

B. Faatz

Deutsches Elektronen Synchrotron DESY, Notkestraße 85, 22603
Hamburg, Deutschland

1   Introduction

In its present design, the TESLA Test Facility FEL, of which the first stage is under construction at DESY, will employ an electron energy of 1 GeV to radiate at a minimum radiation wavelength of 6 nm [1]. Concrete plans exist to use higher harmonic generation to extend this range to 2 nm by using second and third harmonic radiation in a separate, approximately one meter long undulator. The peak power of the radiation in this so-called radiator is a few orders of magnitude smaller than at the fundamental frequency.

The maximum energy of 1 GeV is based on an accelerating gradient of 15 MV/m. Present tests with the first accelerator module indicate the the gradient could possibly be as high as 25 MV/m, the design value for TESLA. Therefore, a moderate extension of the accelerator by two modules would be sufficient to obtain a total energy of the electron beam of 2 GeV instead of the present 1 GeV. This would bring, if all other parameters remain unchanged, the radiation wavelength at the fundamental down to 15Å, but now at a much higher power level than for the 20Å reached with third harmonic generation.

The aim of this report is to investigate what is the possible wavelength range with this extended accelerator. Main points of interest are the required undulator length and the tolerances with respect to undulator errors. The dependence of saturation power and length on undulator parameters is checked in more detail in order to minimize the length of the device.

2   General Considerations

Before performing actual simulations, one can get a feeling for the limits on the FEL performance when increasing the electron beam energy, keeping all remaining parameters fixed. The important quantities are the so-called Pierce parameter ρ [2], the effective energy spread limit [3], the change in shot noise power [4, 5], saturation power and saturation length [6], and the diffraction parameter B [7]. In a one-dimensional limit (i.e. not including the diffraction parameter), they are given by

Table 1: *Parameters of the TTF VUV-FEL: present design for phase II and the upgrades I, II and III*

	Phase II	Upgrade I	II	III
Electron beam				
Energy (GeV)	1	2	2	2
Peak current (kA)	2.5	2.5	2.5	2.5
Norm. emittance (mm mrad)	2π	2π	2π	2π
rms energy spread (%)	0.1	0.05	0.05	0.05
External β-function (m)	3	6	6	3.6
rms electron beam size (μm)	55	55	55	43
Undulator				
Type	Planar	Planar	Planar	Planar
Period (mm)	27.3	27.3	27.3	27.3
Peak magnetic field (T)	0.497	0.497	0.703	0.703
Magnetic gap (mm)	12	12	9.5	9.5
Undulator section length (m)	4.5	4.5	4.5	4.5
Total undulator length (m)	30	60	40	35
Drift section length (mm)	327.6	327.6	327.6	327.6
FODO-lattice				
Period (mm)	955.5	955.5	955.5	955.5
Quadrupole length (mm)	136.5	136.5	136.5	136.5
Quadrupole strength (T/m)	18.3	18.3	18.3	30
Radiation				
Period (nm)	6	1.6	2.3	2.3
Saturation length (m)	25	55.5	36	33

$$\rho = \frac{\lambda_u}{4\pi\ell_g} = \frac{1}{\gamma}\left[\left(\frac{K_{\mathrm{rms}}\lambda_u f_B}{8\pi}\right)^2 \frac{2I_p}{I_A\beta\varepsilon}\right]^{1/3} , \tag{1}$$

where $\gamma = E/mc^2$ is the normalized beam energy, K_{rms} is the rms undulator parameter, λ_u is the undulator period, f_B is the decoupling bessel factor, I_p and I_A are the peak and Alfvén current, respectively, ε is the unnormalized emittance, and $\beta = 2\sigma_{x,y}^2/\varepsilon$, with $\sigma_{x,y}$ the electron beam radius. [1]

$$\hat{\Lambda}_T = \frac{1}{\rho}\left[\left(\frac{\sigma_\gamma}{\gamma}\right)^2 + \left(\frac{\varepsilon\lambda_u}{4\lambda\beta}\right)^2\right]^{1/2} < 1 , \tag{2}$$

with λ the radiation wavelength and σ_γ/γ the relative energy spread.

$$P_{\mathrm{in}} = \frac{3\sqrt{4\pi}\rho^2 P_b}{N_\lambda\sqrt{\ln(N_\lambda/\rho)}} \quad \text{with } P_b = \gamma mc^2 \frac{I_p}{e} \text{ and } N_\lambda = \frac{\lambda I}{ec} , \tag{3}$$

$$P_{\mathrm{sat}} = 1.37 \cdot \rho P_b e^{-0.82\hat{\Lambda}_T^2} , \tag{4}$$

---

[1] There is some arbitraryness in the choice of beam radius depending on the actual shape of the beam. Therefore, the value of $\varepsilon = 2\varepsilon_{\mathrm{rms}}$ is assumed in the calculations that follow for a better comparison with numerical simulations.

with e the elementary charge and ω_0 the resonant radiation frequency. P_b is the electron beam power and N_λ the number of electrons per wavelength. One can see the power reduction at saturation due to energy spread.

$$L_{\text{sat}} = \frac{\lambda_u}{4\sqrt{3}\pi\rho}(1 + \hat{\Lambda}_T^2) \ln \left(\frac{(9 + 6\hat{\Lambda}_T^2)P_{\text{sat}}}{(1 + 6\hat{\Lambda}_T^2)P_{\text{in}}} \right) . \tag{5}$$

Although the diffraction parameter is not used in this analysis, it is given here in order to be complete.

$$B = \frac{16\pi^2 f_B \varepsilon \beta}{\lambda \lambda_u} \left[\frac{I_p}{\gamma I_A} \frac{K_{\text{rms}}^2}{1 + K_{\text{rms}}^2} \right]^{1/2} . \tag{6}$$

The coefficients in front of $\hat{\Lambda}_T$ in Eqs. (4) and (5) have been derived empirically (see Ref. [7]). Although these equations can give a first estimate of the parametric dependence of the FEL, a more accurate procedure solves the FEL dispersion equation, as was done in Ref. [8, 9]. This procedure gives the growth rate of the radiation power. The saturation length can only be determined using Eqs. (3) and (4). With all parameters fixed except for the electron beam energy,
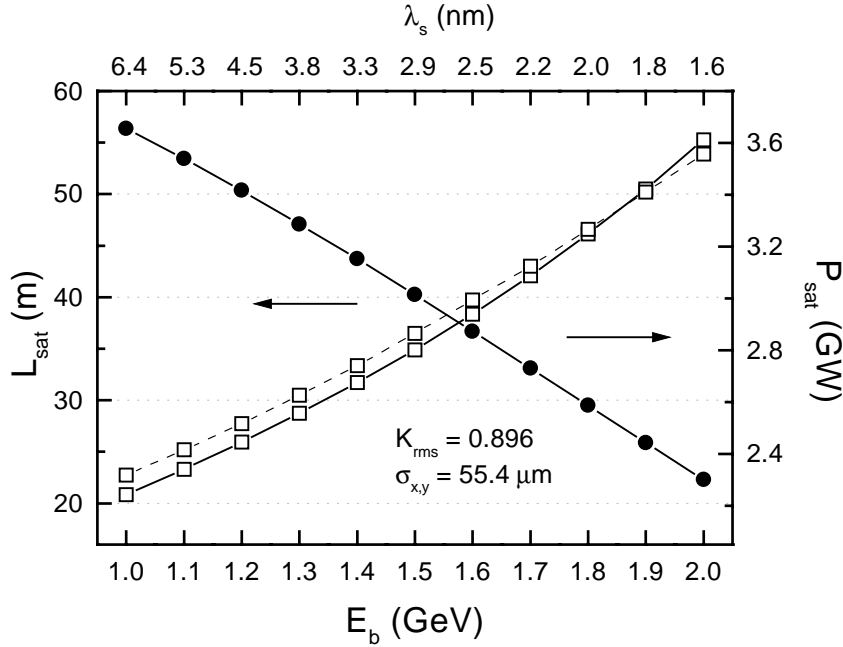

Figure 1: *Saturation length and power as a function of Electron beam energy. All remaining parameters as in Table 1. The solid curves are calculated with Eqs. (4) and (5), the dashed curve is calculated with the dispersion equation together with Eqs. (3) and (4).*

the equations can be rewritten as follows[2] (not taken into account the variation of $\hat{\Lambda}_T$)

$$\rho = \frac{\rho_0}{E_b} , P_{\text{in}} = P_0 \times E_b , P_{\text{sat}} = P_0 , \tag{7}$$

---

[2] Because of the integrated FODO-lattice, the product of β and ε is a constant

$$L_{\text{sat}} = E_b L_0 \left(1 - \frac{\ln(E_b)}{20.5}\right) . \quad B = B_0 \times E_b^{3/2} \tag{8}$$

where the index '0' stands for the values at 1 GeV, 1.7×10^{-3}, 50 W, 4 GW, 23 m and 14 respectively (see Table 1). The beam energy E_b is given in multiples of GeV. Assuming that the longitudinal emittance is conserved, Eq. (2) can be rewritten as

$$\frac{\gamma^2 \varepsilon_n}{\beta(1 + K_{\text{rms}}^2)} < \sqrt{(\gamma\rho)^2 - \sigma_\gamma^2} . \tag{9}$$

The right hand side of this equation is independent of energy. One can easily see that the saturation length is proportional to energy. Even though the effective input power increases with energy, the dependence on this parameter is only logarithmic, whereas the dependence of the saturation length on ρ is linear. In Fig. 1 the saturation length and power are shown as a function of the electron beam energy. The increase in saturation length shows a more than linear dependence due to an increase in $\hat{\Lambda}_T$ (open squares). For the same reason, the power decreases slightly (solid circles). In the same figure, the dashed line gives the saturation length using the dispersive equation as well as the shot noise power and saturation power as determined by Eqs. (3) and (4). The saturation length is virually the same as with Eq. (5). Since the value of the saturation power has been used, this value is obviously the same in both cases.

The diffraction parameter, which ideally has a value close to unity, is rather large for a 2 GeV beam, namely 39. As a consequence, builtup of transverse coherence might be a problem for these parameters. The practical methods of reducing the B-parameter are increasing the undulator period, the radiation wavelength, and decreasing the β-function by increasing quadrupole gradient. The last option has as disadvantage that it increases the effective energy spread, while hardly decreasing the gain length.

Fig. 2 shows results of calculations with an electron beam energy of 2 GeV, where the undulator gap has been decreased, thus increasing the value of the K_{rms}-parameter. Because this enhances the coupling between the electrons and the undulator field (by increasing the transverse component of the electron velocity), the saturation length decreases significantly. In order to have the complete water window available, the wavelength should not increase to values larger than 2.5 nm (see the top scale of Fig. 2). This can be achieved by increasing the K_{rms} value by no more than a factor of 1.4, which is equivalent to decreasing the undulator gap from 12 to 9.5 mm. As can be seen, the saturation length then becomes approximately 33 m for the minimum undulator gap.

For the original undulator gap, the quadrupole gradient could not exceed 25 T/m for the present undulator design. This would give an average β function of 4 m at 2 GeV.[3] For the smaller gap, the average β-function can decrease to 3.6 m. As a consequence, the saturation length decreases to approximately 30 m according to Eq. (5) and 33 m using the dispersion equation, as can be seen in Fig. 3. With these parameters, the diffraction parameter has been reduced to 22, almost a factor of two smaller than before and 50% larger than for the 1 GeV case. Also the effective energy spread has decreased. As can be seen in this figure, the solution using the dispersion equation shows a minimum saturation

[3] for present parameters, the quadrupole gradient is 18.3 T/m, giving rise to an average β-function of 6 m at 2 GeV
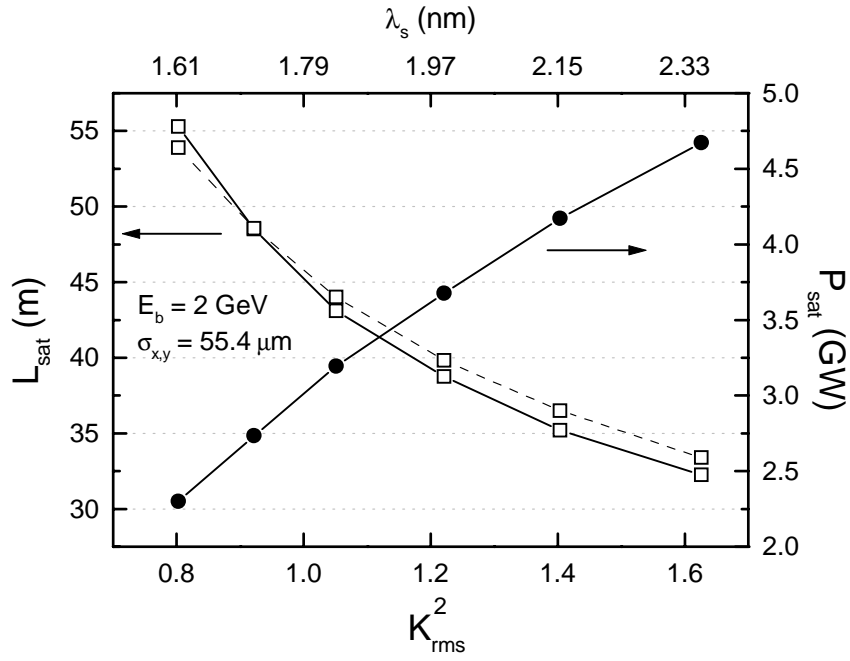
Figure 2: *Saturation power and length at 2 GeV for different values of the K parameter. The solid curves are calculated with Eqs. (4) and (5), the dashed curve is calculated with the dispersion equation.*

length at $\beta = 4.5\,\mathrm{m}$. The minimum calculated with Eq. (5) occurs at $\beta = 3.2\,\mathrm{m}$. This minimum is caused due to a competition between current density and longitudinal velocity spread. The difference between saturation length and and optimum β-function is probably caused by the betatron oscillation, which has been taken into account (partially) in the dispersion equation.

With this system, the undulator FODO-lattice is stable downto electron beam energies of 270 MeV, but a practical limit, given by a maximum variation of the β-function

$$\frac{\beta_{\max}}{\beta_{\min}} \approx \frac{2\overline{\beta} + L_{\mathrm{FODO}}}{2\overline{\beta} - L_{\mathrm{FODO}}} < 3 \qquad (10)$$

is approximately 500 MeV. This maximum value is given by the fact that Eq. (2) has to be obeyed for the smallest value of the β function. Because of the much shorter saturation length at these low energies, this criterium can be relaxed for the given length of the undulator, but the drop in gain for larger values of $\beta_{\max}/\beta_{\min}$ is quite steep and it is unknown what the effect is on the radiation properties. Assuming that 500 MeV is indeed a lower limit, this undulator can be used over a wavelength range exceeding an order of magnitude, e.g. between 35 and 2.3 nm.

Another important issue are magnetic and geometrical undulator errors [10, 11]. Their influence can be described in terms of transverse overlap of the electron beam and the radiation field, given by the second magnetic field integral, and the resonance condition, given by the phase of the electrons with respect to the radiation field of a certain radiation frequency. Although most
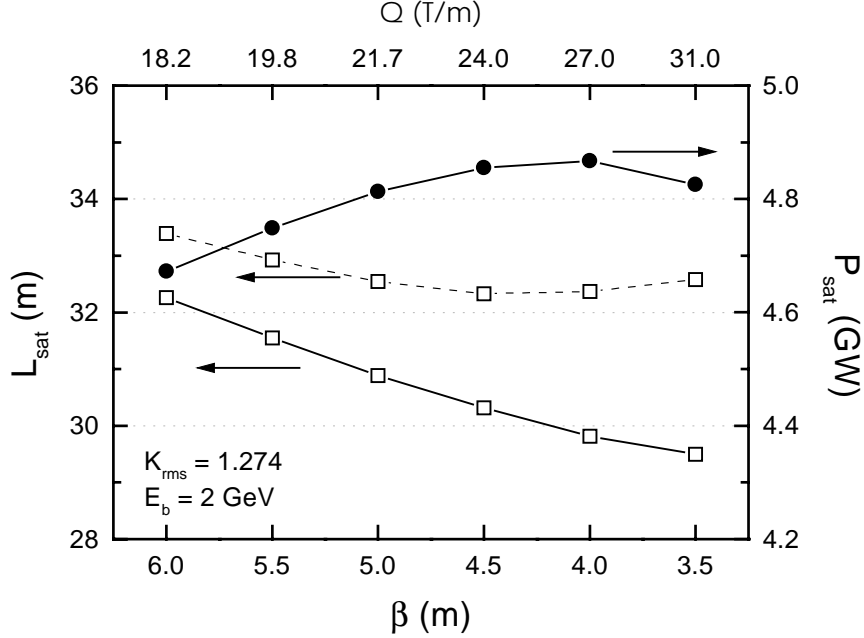
Figure 3: *Saturation length and Power at 2 GeV as a function of the β-function. The radiation wavelength is 2.3 nm The solid curves are calculated with Eqs. (4) and (5), the dashed curve is calculated with the dispersion equation.*

studies so far result in statistical properties of FEL performance reduction due to errors, some general criteria can be derived empirically [11]. The limits on phase shake and on the second field integral are given by

$$\Delta\psi_{\mathrm{rms}} < \frac{1}{\sqrt{3}}\hat{\Lambda}_T \;, \quad I_{2,\mathrm{rms}}(Tmm^2) < 0.65\sigma_{x,y}(\mu m) \times E(GeV) \qquad (11)$$

The distance between correctors in order to correct for beam wander in case of uncorrected field errors of 0.5% or a conservative estimate of a quadrupole misalignment of $\pm\,50\,\mu$m is given by

$$L_D = \min(\ell_g, \beta/2) \;, \qquad\qquad (12)$$

where ℓ_g has been defined in Eq. (1) As can be easily seen, the value for phase shake is independent of energy for upgrade I (see Table 1). In case of upgrades II and III, the phase shake has to decrease in order for phase shake to remain negligible compared to the gain reduction due to energy spread. Although phase shake is not directly related to the rms value of the undulator field error, this statement approximately means that this error has to decrease by the same amount. The demands on the second field integral actually relax with increasing energy if all other parameters are fixed (upgrade I) or when the K_{rms} parameter is increased. For a reduced β-function in the range that has been discussed in Fig. 3, the demands on the second field integral are still mild compared to the (achievable) tolerances needed for the 1 GeV parameters of phase II. Misalignment of individual undulator modules by an amount of Δx leads to a much larger phase shift (after correcting the electron beam position to the

6

undulator center) between electron bunch and radiation field in the inter-module gaps L_G.

$$\Delta L_G = -\frac{(\gamma \Delta x)^2}{L_G} \bmod \lambda_u \ . \tag{13}$$

The requirements on the movement of the undulator does not change however, compared to the present design. In general, the requirements on the undulator design become comparable to the phase II requirements or will be slightly easier to achieve.

3 Numerical simulations

Analytical calculations have given an indication of what one might expect of the behaviour of the FEL when the electron beam energy is increased to 2 GeV. In order to decrease the undulator length , the two options discussed in more detail are to increase the K_{rms} parameter and/or the quadrupole gradient. It should be stressed that the modifications to the undulator are only minor, none of them in the fundamental design. For the parameters given in Table 1, a number of simulations have been performed. Compared to the analytical
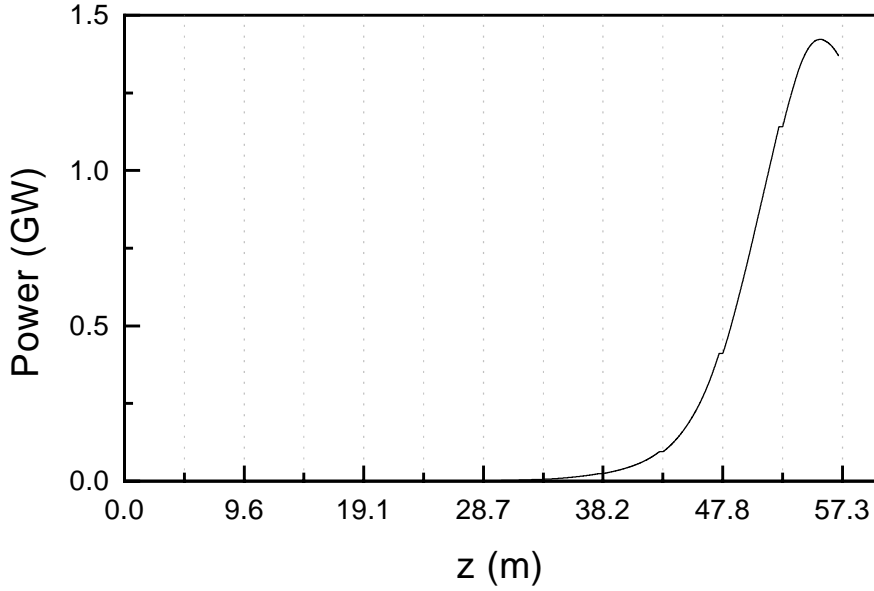

Figure 4: *Power along the undulator for the parameters given in table 1, upgrade I.*

calculations presented in the previous section, the simulations performed here take into account the discrete FODO lattice, including the variation of the β function. For the simulations, a 3-dimensional, steady state simulation code has been used [12, 13]. The effective input power is taken equal to the value of P_{in} calculated with Eq. (4) in a single Gaussian mode.

Fig. 4 shows the power growth along the undulator with only the electron beam energy increased. Due to the modular configuration of the undulator with 300 mm of field free space in between, the power is constant at certain positions.
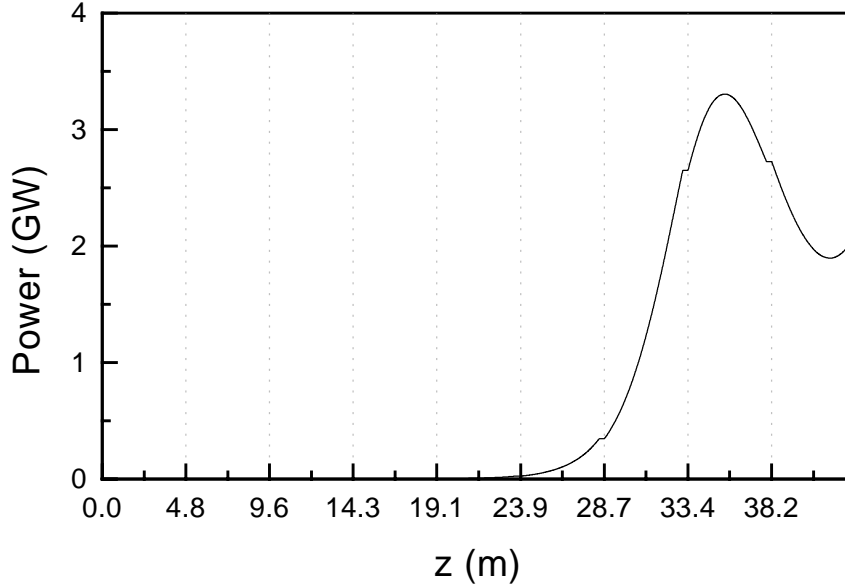
Figure 5: *Power along the undulator for the parameters given in table 1, upgrade II.*

The gain length is approximately 2.9 m. The gain length calculated from the ρ parameter is 2.82 m, including the effective energy spread $\hat{\Lambda}_T$. The saturation length is approximately 55.5 m, including the 3.3 m reserved for diagnostics. The saturation power is 1.5 GW, which is a factor of two smaller than the power obtained in the previous section. The reduction can be caused either by the large value of the diffraction parameter B, or by the fact the the emittance is very close to the tolerable limit (see Eq. (9)), thus making the approximation less accurate.

In Fig. 5, the power growth along the undulator is shown for an increased K_{rms}-parameter of 1.267. The radiation wavelength is 2.3 nm in this case. Due to the increased interaction, the saturation length is 35 m, a reduction of 40% compared to the result shown in the previous figure. This reduction of saturation length results in an undulator consisting of 8 undulator modules instead of the 12 needed in the previous simulation. At the same time, the diffraction parameter has been reduced from 50 to 27.5, and hence the problems expected with the builtup of transverse coherence are reduced. The saturation power is close to the 4 GW calculated analytically.

In Fig. 6, in addition to increasing the K_{rms}-parameter, the β-fuction is smaller due to an increase of the quadrupole gradient to 30 T/m. This again decreases the B-parameter. The effective energy spread has become larger, however. As a result, the reduction in saturation length is only moderate. The benefit is that an undulator of 7 modules is needed in this case, only one more than the foreseen 6 modules for the 1 GeV design. The saturation power has decreased compared to the previous simulation. The analytical calculation predicted a further increase in power. The reason for this discrepancy is not known.
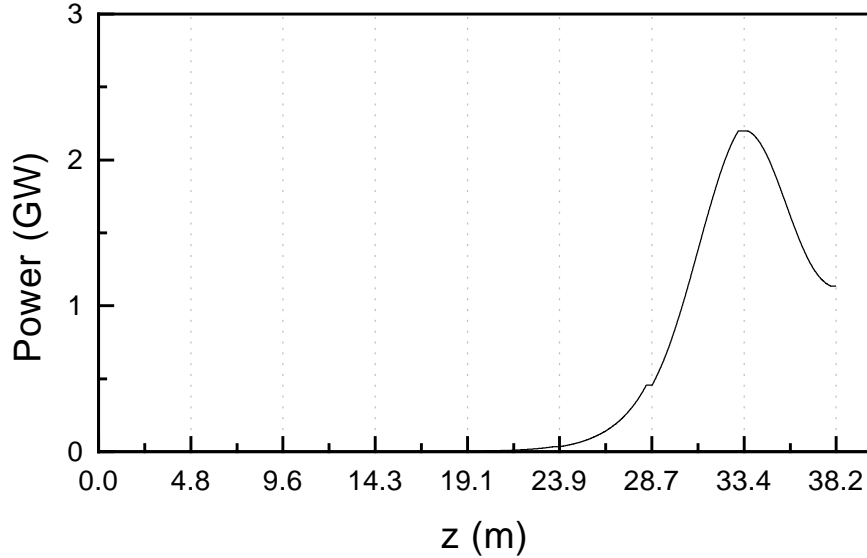
Figure 6: *Power along the undulator for the parameters given in table 1, upgrade III.*

Higher harmonic generation

For these last undulator parameters, the second and third harmonic is calculated in case the electron beam is sent through a radiator. Results are shown in Fig. 7. Because the radiation in the first undulator saturates very close to the undulator exit, an eight module has been assumed for these simulations. Because the bunching in this last module is reduced by a factor two due to the induced energy spread, the power given is a lower estimate. The divergence of the electron beam has been reduced by changing the gradient of the last quadrupole from 30 to 15 T/m. The radiator has a planar geometry with a period of 12 mm without quadrupole focusing. For the second harmonic (where the largest undulator field strength is required) the peak field is 1.78 T, which is feasible with superconducting technology.

4 Reaching the water window with lower electron beam energies.

Although the study in this paper assumes that a 2 GeV electron beam is available, one does not need this energy to include the water window in the wavelength range of the TTF-FEL. Fig. 8 shows the dependence of the saturation length on the energy, keeping the radiation wavelength fixed at 2.3 nm by simultaneously changing the undulator gap. The results are obtained using Eq. (5). Because the space that can be used is limited, the combined length of accelerator modules and undulator is fixed. Reducing the accelerator by one module saves approximately 12 m, an undulator module has a length of 4.5 m. One could therefore choose to reduce the accelerator by one module, thus reducing the beam energy by 200 MeV, adding one or two undulator modules to reach
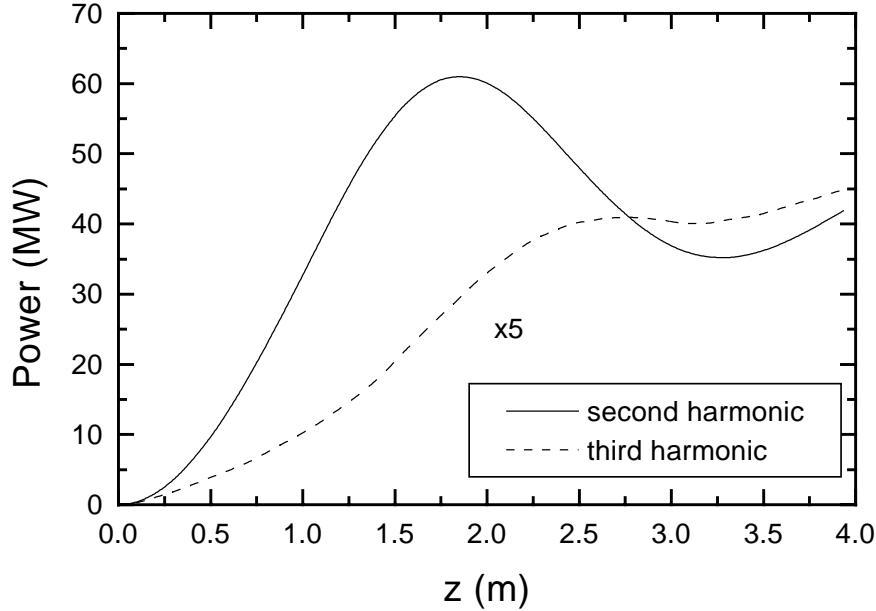
9

Figure 7: *Power along the undulator for the second and third harmonic in a radiator behind the first undulator. The third harmonic power has been multiplied by 5.*

saturation. This would reduce the price of the system, since a superconducting accelerator module is more expensive than two undulator modules, and still leave an additional 3 m of space for diagnostics or a radiator for higher harmonic generation. The estimated reduction in saturation power is a mere factor of two.

5 Conclusions

Both analytical calculations and simulations have shown that if all parameters are fixed except for the beam energy, the saturation length for a 2 GeV electron beam is approximately 55 m, e.g., twice the length needed for the 1 GeV energy with a four times longer wavelength. The main worry is the large B parameter, which could indicate that the system has difficulty developing full transverse coherence.

The best method to shorten the undulator is to improve the electron beam quality. In case this is not possible, the undulator design has to be changed for the 2 GeV case. Increasing the K_{rms} parameter by a factor 1.4 by decreasing the undulator gap from 12 to 9.5 mm results in a radiation wavelength of 2.3 nm, which would still bring the water window within the wavelength range. In this case the saturation length limits the undulator length to 8 undulator modules of 4.5 m. A further reduction by one module is possible by increasing the focusing strength. This limits the minimum electron beam energy that can be used to approximately 500 MeV. For values smaller than this energy the variation of the β functions becomes large. Below 300 MeV the phase advance per FODO
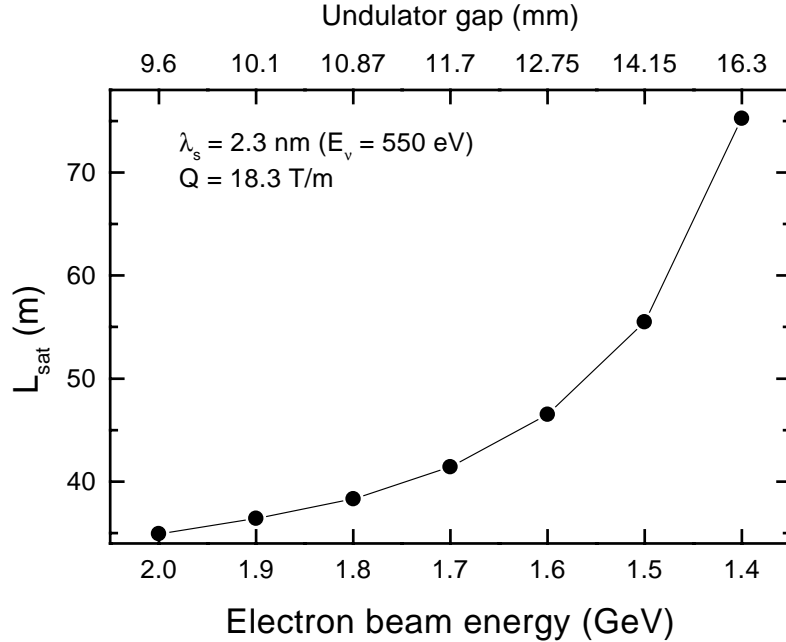
Undulator gap (mm)

Figure 8: *Saturation power with changing electron beam energy, keeping the radiation wavelength constant at 2.3 nm by simultaneously changing the undulator gap.*

period becomes too large and the focusing structure becomes unstable.

The sensitivity to undulator errors does not change drastically. The demand on the magnetic undulator errors becomes slightly tighter, whereas the required second field integral can be relaxed.

Both analytical calculations and simulations have been performed neglecting the effect of resistive wall wake-fields. Increasing the energy would make this effect smaller. Once the undulator gap is reduced, the effect might result in a measurable reduction in gain, especially if this undulator is also used at lower energies. More detailed simulations are needed to study this effect. Also the large diffraction parameter B, and the builtup of transverse modes, has not been studied. A simulation code taking into account the transverse shot noise has to investigate this effect.

References

[1] *"A VUV Free Electron Laser at the TESLA Test Facility: Conceptual Design Report"*, DESY Print TESLA-FEL 95-03, Hamburg, DESY, 1995.

[2] R. Bonifacio, C. Pellegrini and L.M. Narducci Optics Commun. **53** (1985) 197.

11

[3] J. Roßbach, E.L. Saldin, E.A. Schneidmiller and M.V. Yurkov, Nucl. Instr. and Meth. **A393** (1997) 152.

[4] R. Bonifacio, L. De Salvo, P. Pierini, N. Piovella and C. Pellegrini Phys. Rev. Letters **73** (1994) 70.

[5] E.L. Saldin, E.A. Schneidmiller and M.V. Yurkov, Nucl. Instr. and Meth. **A393** (1997) 157.

[6] A.M. Kondratenko and E.L. Saldin, Particle Accelerators, **10** (1980) 207.

[7] E.L. Saldin, E.A. Schneidmiller and M.V. Yurkov, Physics reports **260** (1995) 187-327.

[8] L.H. Yu, C.M. Hung, D. Li and S. Krinsky Phys. Rev E **51** (1995) 813.

[9] L.H Yu, S. Krinski, R.L. Gluckstern, Phys. Rev Lett. **64** (1990) 3011.

[10] L.H. Yu, S. Krinski, R.L. Gluckstern and J.B.J. Zeijts, Phys. Rev. A45 (1992) 1163.

[11] B. Faatz, J. Pflüger and Yu.M. Nikitina, Nucl. Instr. and Meth. **A393** (1997) 380.

[12] T.-M. Tran and J.S. Wurtele, Comp. Phys. Commun. **54** (1989) 263.

[13] P. Jha and J.S. Wurtele, Nucl. Instr. and Meth. **A331** (1993) 477.